© 2015. Published by The Company of Biologists Ltd | Journal of Cell Science (2015) 128, 1639–1653 doi:10.1242/jcs.163279

RESEARCH ARTICLE

Nek2A destruction marks APC/C activation at the prophase-to-prometaphase transition by spindle-checkpoint-restricted Cdc20

Michiel Boekhout[1] and Rob Wolthuis[1,2,*]

ABSTRACT

Nek2 isoform A (Nek2A) is a presumed substrate of the anaphase-promoting complex/cyclosome containing Cdc20 (APC/C^{Cdc20}). Nek2A, like cyclin A, is degraded in mitosis while the spindle checkpoint is active. Cyclin A prevents spindle checkpoint proteins from binding to Cdc20 and is recruited to the APC/C in prometaphase. We found that Nek2A and cyclin A avoid being stabilized by the spindle checkpoint in different ways. First, enhancing mitotic checkpoint complex (MCC) formation by nocodazole treatment inhibited the degradation of geminin and cyclin A, whereas Nek2A disappeared at a normal rate. Second, depleting Cdc20 effectively stabilized cyclin A but not Nek2A. Nevertheless, Nek2A destruction crucially depended on Cdc20 binding to the APC/C. Third, in contrast to cyclin A, Nek2A was recruited to the APC/C before the start of mitosis. Interestingly, the spindle checkpoint very effectively stabilized an APC/C-binding mutant of Nek2A, which required the Nek2A KEN box. Apparently, in cells, the spindle checkpoint primarily prevents Cdc20 from binding destruction motifs. Nek2A disappearance marks the prophase-to-prometaphase transition, when Cdc20, regardless of the spindle checkpoint, activates the APC/C. However, Mad2 depletion accelerated Nek2A destruction, showing that spindle checkpoint release further increases APC/C^{Cdc20} catalytic activity.

KEY WORDS: APC/C, Cdc20, Cyclin A, Nek2A, Spindle checkpoint

INTRODUCTION

The anaphase-promoting complex/cyclosome (APC/C) is an E3 ubiquitin ligase that, together with either one of its regulatory co-activators, Cdc20 or Cdh1, targets multiple mitotic regulators for proteasomal degradation. These include cyclin B1, securin and geminin, making APC/C^{Cdc20} a major factor in directing cell division, sister chromatid separation and DNA replication licensing (Clijsters et al., 2013; Peters, 2006; Pines, 2011). Several questions remain about how the activity of APC/C^{Cdc20} is controlled in mitosis. Phosphorylation of the APC/C by mitotic kinases at the end of prophase leads to an increased affinity for Cdc20 (Kramer et al., 2000; Yudkovsky et al., 2000). The formation of the complex between the APC/C and co-activator probably induces a conformational change that activates the APC/C (Dube et al., 2005; Kimata et al., 2008), perhaps by facilitating the recruitment of the E2 enzyme UbcH10 (Chang et al., 2014; Van Voorhis and Morgan, 2014). Cdc20 also acts as an APC/C substrate recruitment factor that binds directly to degradation motifs in APC/C substrates, such as the D-box and the KEN box (da Fonseca et al., 2011; Kraft et al., 2005). At the point in the cell cycle when APC/C^{Cdc20} complexes are formed, however, the spindle checkpoint also becomes active and blocks Cdc20. Spindle checkpoint proteins, including Mad2 and BubR1, capture Cdc20 into the inhibitory mitotic checkpoint complex (MCC) (Chao et al., 2012). Cdc20 remains inhibited by the spindle checkpoint until the chromosomes are bi-oriented on the mitotic spindle (Foley and Kapoor, 2013; Kim and Yu, 2011; Lara-Gonzalez et al., 2012). Once the spindle checkpoint is satisfied, APC/C^{Cdc20} becomes active and sends cyclin B1, securin and geminin for proteasomal degradation (Clijsters et al., 2013; Clute and Pines, 1999; Hagting et al., 2002). Interestingly, however, the APC/C^{Cdc20} substrate cyclin A2 disappears shortly after nuclear envelope breakdown, regardless of the inhibitory effect of the spindle checkpoint (den Elzen and Pines, 2001; Geley et al., 2001).

The mechanism by which cyclin A destruction evades the spindle checkpoint has largely been solved. The N-terminus of cyclin A associates strongly with Cdc20 and thereby competes off the spindle checkpoint proteins (Di Fiore and Pines, 2010; van Zon et al., 2010; Wolthuis et al., 2008). Thus, cyclin A, by its N-terminus, binds a specific fraction of Cdc20 that cannot be blocked by Mad2 and BubR1. In addition, the Cdc20–cyclin-A complex, bound to Cdk1 and Cks, is exclusively recruited to the APC/C in prometaphase, when the APC/C becomes phosphorylated (Wolthuis et al., 2008). Recently, it has been shown that cyclin A destruction early in mitosis is necessary for progressive stabilization of the mitotic spindle, promoting proper attachments to kinetochores and formation of the metaphase plate (Kabeche and Compton, 2013).

Nek2 isoform A (Nek2A) is a centrosomal kinase that is highly expressed in G2 phase but rapidly disappears in prometaphase. Nek2A phosphorylates, for instance, C-Nap and Rootletin, which are involved in centrosome separation and bipolar spindle formation (Bahe et al., 2005; Bahmanyar et al., 2008; Fry et al., 1998a; Fry et al., 1998b), but more recently it has also been implicated in the Hippo signalling pathway (Mardin et al., 2010). Although Nek2A is an APC/C substrate, conclusive evidence that its destruction in mammalian cells depends only on APC/C^{Cdc20}, or that a different proteasomal targeting pathway contributes to its degradation, too, is lacking. Furthermore, the role of Cdc20 in directing APC/C-mediated Nek2A degradation is under debate (Kimata et al., 2008; Sedgwick et al., 2013). In contrast to cyclin A, even at high levels Nek2A, has not been found to interfere with the ability of BubR1 to bind Cdc20 (Sedgwick et al., 2013), indicating that Nek2A and cyclin A might differ in the way their destruction escapes control by the spindle checkpoint. Because

[1]Division of Cell Biology I (B5) and Division of Molecular Carcinogenesis (B7), The Netherlands Cancer Institute (NKI-AvL), 1066 CX Amsterdam, The Netherlands. [2]Department of Clinical Genetics (Division of Oncogenetics), VUmc and VUmc Cancer Center Amsterdam, CCA/V-ICI Research Program Oncogenesis, VUmc Medical Faculty, 1081 HV Amsterdam, The Netherlands.

*Author for correspondence (r.wolthuis@vumc.nl)

Received 12 September 2014; Accepted 6 February 2015

Journal of Cell Science (2015) 128, 1639–1653 doi:10.1242/jcs.163279

the spindle checkpoint might block the recruitment of substrates to the APC/C by Cdc20, an attractive model explaining the timing of Nek2A degradation is that its destruction depends only on the APC/C, not on Cdc20. An observation in support of this model is that Nek2A has a C-terminal MR tail that binds directly to the TPR motifs of APC/C subunits (Hames et al., 2001; Hayes et al., 2006; Sedgwick et al., 2013). However, in such a model, Nek2A binding to the APC/C would be expected to be regulated by the cell cycle, to explain its timely destruction. Furthermore, a TPR-binding tail is, for instance, also present in the stable APC/C component APC10, showing that this motif alone is insufficient to turn a protein into an APC/C substrate (Wendt et al., 2001; Vodermaier et al., 2003; Matyskiela and Morgan, 2009). Nek2A forms dimers that facilitate Nek2A binding to the APC/C (Sedgwick et al., 2013), but dimerization is also not regulated by the cell cycle (Fry et al., 1999). Taken together, therefore, it is unclear which mechanism ensures that Nek2A is degraded at the right time in mitosis and what the role of Cdc20 is in this process. Here, we tried to address this by asking whether Nek2A turnover relies exclusively on the APC/C and Cdc20, and, how Nek2A degradation escapes control by the spindle checkpoint. We analyzed Nek2A degradation in live cells in relation to two well-characterized APC/C^{Cdc20} substrates, geminin, which is stabilized in response to the spindle checkpoint, and cyclin A, which is degraded independently of the spindle checkpoint.

RESULTS

Nek2A is degraded in mitosis regardless of enforced spindle checkpoint activation

As detected by western blotting, Nek2A is degraded when cells are arrested in mitosis by taxol treatment (Fig. 1A). We wanted to know whether, as was reported recently for cyclin A, Nek2A might be partially stabilized by increasing the formation of the Cdc20-inhibitory MCC, a consequence of treating mitotic cells with spindle poisons (Collin et al., 2013; Westhorpe et al., 2011). To follow detailed changes in protein stability over time, we used time-lapse fluorescence microscopy of U2OS cells expressing geminin–Cherry, a validated checkpoint-controlled APC/C^{Cdc20} substrate (Clijsters et al., 2013), together with an N-terminally tagged Venus–Nek2A fusion, during G2 phase and mitosis (Fig. 1B). Upon nocodazole treatment, geminin–Cherry remained stable as long as cells delayed in mitosis (Fig. 1C). However, fluorescent Nek2A was destroyed right at the prophase-to-prometaphase transition, regardless of whether cells were left untreated or were blocked by either nocodazole or taxol (Fig. 1C,D; supplementary material Fig. S1A shows the expression levels of the fluorescent Nek2; also see Fig. 3B, below). We conclude therefore that Nek2A differs from other APC/C^{Cdc20} substrates, including cyclin A, in that its degradation is not delayed at all by increasing spindle checkpoint activity. These results indicate that Nek2A is either not exclusively degraded by APC/C^{Cdc20}, or that Nek2A destruction occurs regardless of whether Cdc20 is blocked by spindle checkpoint proteins or not.

Nek2A degradation after inhibiting APC/C^{Cdc20}

To resolve this matter, we first investigated whether Nek2A degradation exclusively depended on Cdc20. We used time-lapse fluorescence microscopy to follow cells stably expressing both geminin–Cherry and Venus–Nek2A, after treatment with small interfering RNA (siRNA) directed against Cdc20. In control cells, Venus–Nek2A destruction started right at nuclear envelope breakdown (NEBD) [Fig. 2A, top panel, Fig. 2B; fluorescent Nek2A protein levels reached 50% of their NEBD levels within 15.6±6.1 min (mean±s.d.), n=25, in three independent experiments]. Although the mitotic delay after Cdc20 siRNA varied between cells, we found that cells arresting in mitosis for 2 h or more did not degrade geminin–Cherry. Remarkably however, fluorescent Nek2A was degraded only slightly more slowly (Fig. 2A, middle panel, Fig. 2C). In these cells, the point when 50% of fluorescent Nek2A had disappeared was delayed to 28.5±12.0 min (mean±s.d., n=47, five independent experiments, Fig. 2C). We then investigated the effect of the APC/C inhibitor ProTAME, which blocks normal binding of Cdc20 to the APC/C (Zeng and King, 2012; Zeng et al., 2010). Although treatment with 20 µM of ProTAME almost completely stabilized geminin–Cherry, we observed only modest stabilization of Venus–Nek2A, roughly similar to the partial stabilization of Venus–Nek2A following Cdc20 siRNA (half-life 41±12.6 min; mean±s.d., n=15 from two independent experiments, Fig. 2A, bottom panel; Fig. 2D). When depleting the cullin-like subunit APC2, NEBD to anaphase lasted 489.1±200 min (n=13 from three independent experiments). In addition, in these cells, geminin–Cherry was clearly stabilized, confirming efficient depletion of the APC2 subunit (Fig. 2E, western blot inset). Nevertheless, Venus–Nek2A was still degraded effectively (Fig. 2E; time to 50% of the Venus–Nek2A levels at NEBD was 17.8±3.6 min, mean±s.d.). Significant stabilization of Venus–Nek2A was not observed in APC3 siRNA cells or after the combined knockdown of Ube2S and UbcH10, even though geminin–Cherry was largely stable in these cells (supplementary material Fig. S1B,C, respectively). Endogenous Nek2A also disappeared despite depletion of APC subunits or the APC/C-directed E2 enzyme Ube2S (supplementary material Fig. S1D). Hence, Nek2A degradation proceeds even when the function of APC/C^{Cdc20} is significantly impaired. This indicates that a second, APC/C^{Cdc20}-independent, pathway targets Nek2A under these conditions. Alternatively, a catalytic amount of APC/C^{Cdc20}, remaining after either APC subunit or Cdc20 depletion by RNAi, or after pharmacological inhibition of APC/C^{Cdc20}, is sufficient to effectively process Nek2A.

Cyclin A destruction is more dependent on Cdc20 than Nek2A destruction

We then directly compared the degradation of Nek2A to that of the spindle-checkpoint-independent APC/C^{Cdc20} substrate cyclin A in live cells. We made use of tetracyclin-inducible cyclin-A–Venus U2OS cells stably expressing Cherry–Nek2A. During unperturbed mitosis, or after nocodazole treatment, Nek2A degradation started several minutes before that of cyclin A, exactly at the point of NEBD, as determined by the abrupt appearance of cytoplasmic cyclin A (Fig. 3A, top panel, Fig. 3A,B, destruction plots). Nek2A degradation progressed more rapidly than that of cyclin A (Fig. 3A, destruction plot). Typically, we had found that Cdc20 needs to be depleted to below 5% of its normal cellular levels for cyclin A stabilization (Wolthuis et al., 2008). In a Cdc20 RNAi experiment where the time from NEBD to anaphase was 183 min ±72.9 s.d., and 50% of cyclin-A–Venus remained after 74 min of mitotic delay, Cherry–Nek2A was only minimally stabilized (Fig. 3C, supplementary material Fig. S2A). In another experiment that led to more severe Cdc20 depletion, NEBD to anaphase lasted more than 12 h (766.5±152.3 min, mean±s.d., supplementary material Fig. S2B). However, although these Cdc20 siRNA cells failed to degrade cyclin A for the first 120 min of mitosis, Nek2A still declined rapidly (Fig. 3D). Apparently, depleting Cdc20

Journal of Cell Science (2015) 128, 1639–1653 doi:10.1242/jcs.163279

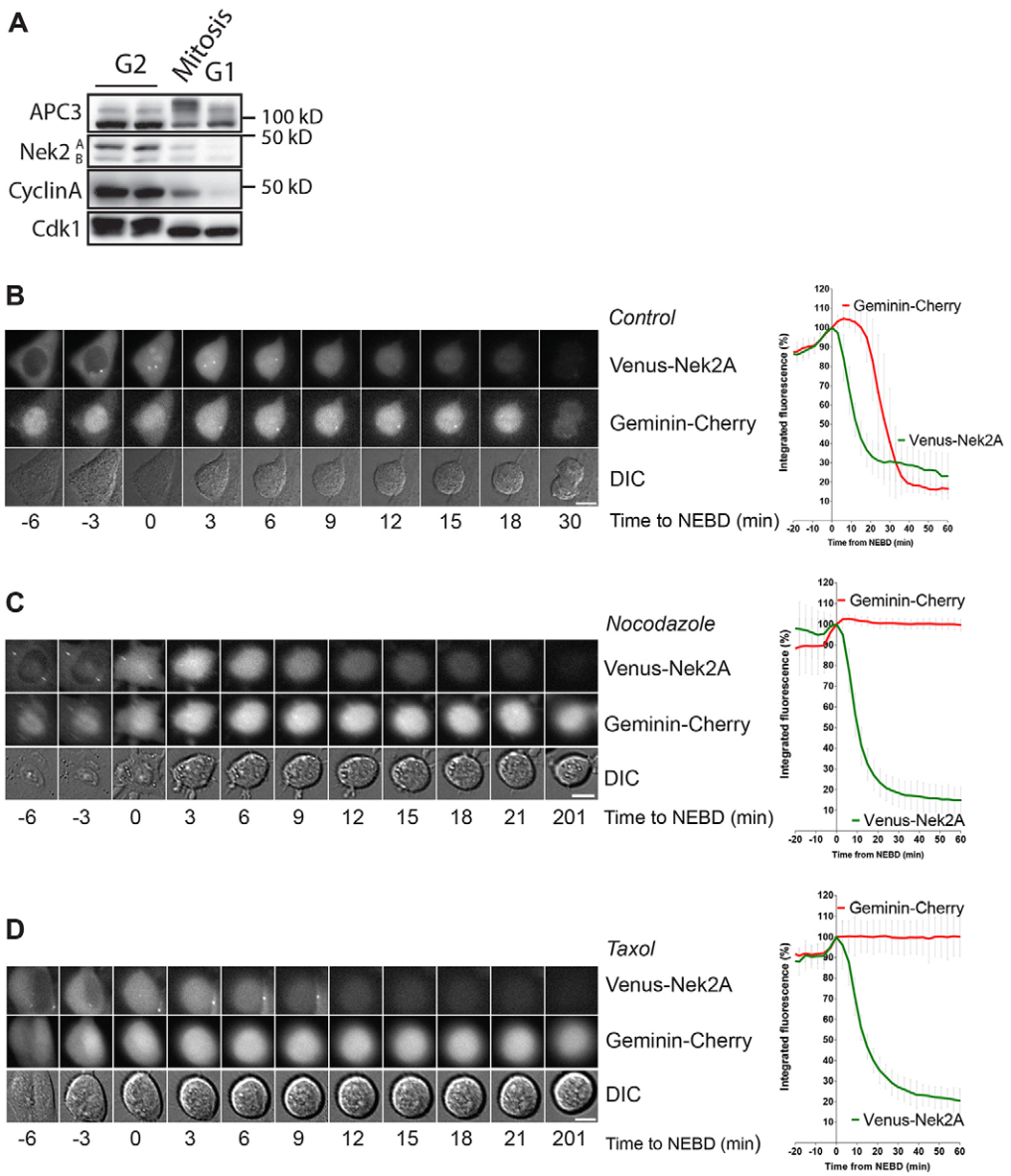

Fig. 1. Nek2A destruction does not respond to super-activation of the spindle checkpoint. (A) U2OS cells were synchronized in G2-phase by an 8-h thymidine release (G2) or were released into taxol after a 24-h thymidine block followed by collection of mitotic cells after 16 h by 'shake off' (Mitosis). Mitotic cells were treated for 1 h with roscovotine to force them out of mitosis into a G1-like state (Skoufias et al., 2007) (G1). Lysates were then prepared and analyzed by western blotting. (B) U2OS cells stably transduced with retroviral Venus–Nek2A and Geminin–Cherry constructs and were imaged by fluorescence and DIC time-lapse microscopy at 3-min intervals. The images show degradation of Nek2A and geminin during a normal mitosis. (C) Nocodazole-treated cells and (D) taxol-treated cells degrade Nek2A at rates normal for mitosis, showing that Nek2A degradation does not respond to the increased spindle checkpoint activity under conditions of treatment with spindle poisons. Integrated fluorescence of the cells was measured and normalized to the intensities in the frame when NEBD started (set at 100%), as determined by the first detection of cytoplasmic dispersal of nuclear geminin–Cherry. Graphs shown are mean±s.d. (n=7 from two independent experiments). Scale bars: 10 µm.

affects cyclin A destruction much more than Nek2A destruction (Fig. 3C,D; supplementary material Fig. S2A,B). Nevertheless, the degree to which Nek2A was stabilized correlated with the degree of cyclin A stabilization upon Cdc20 depletion. Similar results were obtained when we followed cells depleted for either APC2 or the combination of E2 enzymes, Ube2S and UbcH10 (supplementary material Fig. S2C,D). These results again suggest that Nek2A can either be processed independently of the APC/C or Cdc20, or that a very small amount of Cdc20, remaining after siRNA treatment, is sufficient to support Nek2A degradation. To fully block the function of Cdc20, we then combined Cdc20 siRNA with proTAME, which act synergistically (Zeng et al., 2010). Interestingly, both cyclin-A–Venus and Cherry–Nek2A became completely stable during prometaphase (compare Fig. 3E, proTAME alone, with Fig. 3F, proTAME plus Cdc20 siRNA). ProTAME, a cell-permeable compound that resembles an IR tail, did not interfere with the recruitment of Nek2A to the APC/C (supplementary material Fig. S3A,B, and see below). This shows that Nek2A destruction in mitosis fully depends on binding of Cdc20 to the APC/C. We propose that, although processing of cyclin A by the APC/C requires stoichiometric cyclin-A–Cdc20 complexes, Nek2A degradation is directed by a catalytic effect of Cdc20 on the APC/C that immediately springs into action at the prophase-to-prometaphase transition.

Journal of Cell Science (2015) 128, 1639–1653 doi:10.1242/jcs.163279

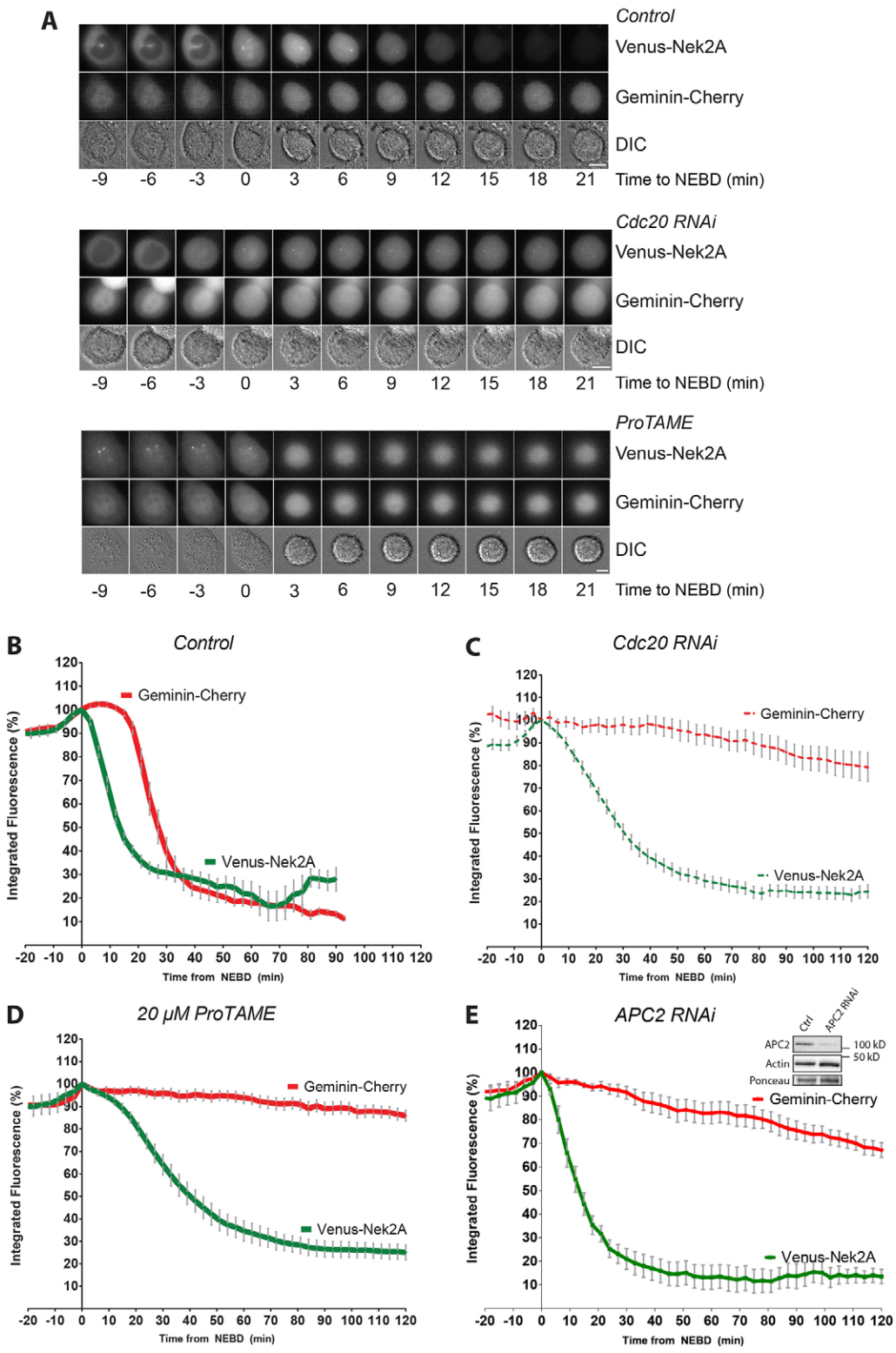

Fig. 2. Compared to the spindle checkpoint-dependent APC/C^{Cdc20} substrate geminin, Nek2A is not efficiently stabilized by direct inhibition of APC/C^{Cdc20}. (A) U2OS cells were imaged by fluorescent and DIC microscopy at 3-min intervals, after treatment with siRNA oligonucleotides (RNAi) or ProTAME as indicated. The time on the *x*-axis was set to 0 at the onset of NEBD, as explained in the legend to Fig. 1. Scale bars: 10 µm. (B–D) Mean±s.e.m. fluorescence intensities for multiple single cells are shown (fluorescence was normalized to 100% fluorescence for $t=0$). (B) Control cells, $n=20$ from three separate experiments; (C) U2OS cells treated with Cdc20 siRNA, $n=47$ from four separate experiments; (D) U2OS cells treated 20 µM ProTAME, $n=15$ from two independent experiment. (E) U2OS cells stably expressing the indicated fusion proteins were transfected with APC2 siRNA and were either used for imaging analysis as in B or lysed and analyzed by western blotting (inset). Graph depicts mean±s.e.m. values, $n=13$ from three separate experiments.

Nek2A is recruited to the APC/C in interphase as well as in mitosis

Previous *in vitro* work has shown that Nek2A can bind directly to the APC/C even in the absence of Cdc20 (Hayes et al., 2006). To explain the sudden disappearance of Nek2A when cells enter mitosis, we hypothesized that Nek2A recruitment to the APC/C might be regulated by the cell cycle. We compared binding of Nek2A to the APC/C in extracts from cells synchronized in G2 phase or in mitosis. To stabilize Nek2A, we arrested cells in nocodazole and added the proteasome inhibitor MG132. Surprisingly, Nek2A bound strongly to the APC/C in G2 phase, as well as in mitosis (Fig. 4A,B, APC4 immunoprecipitations; supplementary material Fig. S3C shows validation of the specificity of the detected Nek2A and Nek2B bands). Low

Journal of Cell Science (2015) 128, 1639–1653 doi:10.1242/jcs.163279

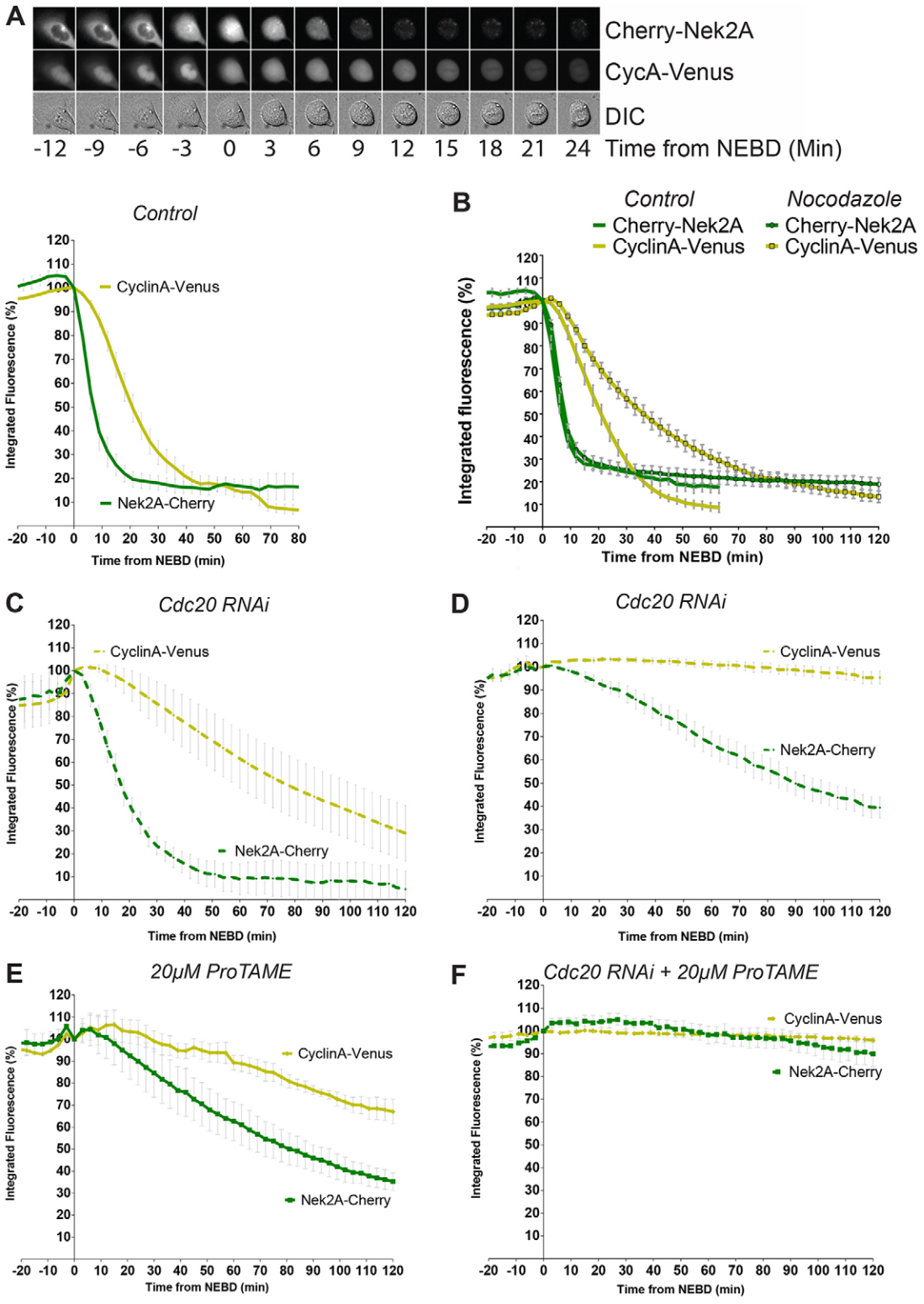

Fig. 3. See next page for legend.

levels of Nek2A protein were also detected in Cdc20 immunoprecipitations, together with the APC/C (Fig. 4B, Cdc20 immunoprecipitations). Whereas Mad2 bound predominantly to mitotic APC/C^{Cdc20}, Nek2A similarly bound G2-phase or mitotic APC/C^{Cdc20} (Fig. 4B). Apparently, and in contrast to cyclin A, Nek2A is recruited to the APC/C in interphase, before it gets degraded in mitosis. Furthermore, APC/C-binding of Nek2A occurred independently of Cdc20 or Cdh1 (Fig. 4C; Hayes et al., 2006; Kimata et al., 2008). Cdc20 or Cdh1 depletion did not affect binding of Nek2A to the G2-phase APC/C, indicating there is no

Journal of Cell Science

Journal of Cell Science (2015) 128, 1639–1653 doi:10.1242/jcs.163279

Fig. 3. Compared to the spindle checkpoint-independent APC/C^{Cdc20} substrate cyclin A, Nek2A is not effectively stabilized by depletion of Cdc20. (A) Montage of U2OS cells expressing TET-inducible cyclin-A2–Venus, also stably expressing Cherry–Nek2A. Cells were imaged during normal mitotic progression. Integrated fluorescence for both fusion constructs was measured and plotted as in Fig. 1B (solid lines, n=10). (B) U2OS cells were synchronized with thymidine and release, after which tetracycline was added to induce cyclin-A–Venus expression. Nocodazole was added 6 h after release and cells were imaged at 3-min intervals. Symbol free lines are control cells (n=15, three separate experiments); dark symbols indicate nocodazole-treated cells (n=15 3 separate experiments). Results are mean±s.e.m. (C) U2OS cells were treated with Cdc20 siRNA (RNAi) (dotted line, n=8), synchronized with thymidine and treated with tetracycline after thymidine release to induce cyclin-A–Venus expression. See also supplementary material Fig. S2A. (D) U2OS cells were treated with Cdc20 siRNA (dotted line n=11). Cells were synchronized with thymidine after transfection, and released in the presence of tetracycline to induce cyclin-A–Venus expression. Efficiency of the knockdown is revealed in a single-cell manner by the stability of cyclin-A–Venus during the first 120 min of the mitotic delay and greatly increased time from NEBD to anaphase. See also supplementary material Fig. S2B. (E) Similar to B, but cells were treated with ProTAME for 6 h after thymidine release. (F) U2OS cells were transfected with Cdc20 siRNA as in D, but ProTAME was added 6 h after thymidine release before imaging by fluorescence and DIC microscopy at 3-min intervals.

competition between co-activators and Nek2A for APC/C binding, nor is there a clear stimulatory effect of the co-activators on recruitment of Nek2A to the APC/C (Fig. 4C). This shows that degradation of Nek2A is not initiated by its increased binding to APC/C^{Cdc20} and implies that the start of Nek2A degradation, which we show is entirely APC/C^{Cdc20} dependent, reflects the exact moment when Cdc20 activates the APC/C.

For its timely degradation, cyclin A needs to compete Mad2 and/or BubR1 away from Cdc20 (Wolthuis et al., 2008; van Zon et al., 2010; Di Fiore and Pines, 2010). However, in nocodazole-arrested cells treated with MG132 after mitotic shake-off, we found that Nek2A is in complex with Cdc20 as well as Mad2 (Fig. 4D). Furthermore, in BubR1 immunoprecipitations of mitotic cells treated with nocodazole and, treated with MG132 after mitotic shake-off, we detected APC/C, Cdc20 and Nek2A (Fig. 4E,F). This is in agreement with earlier *in vitro* experiments showing that Nek2A does not interfere with BubR1–Cdc20 complex formation (Sedgwick et al., 2013). Although both Nek2A and checkpoint proteins bound to the APC/C, only a small amount of Nek2A re-accumulated on the MCC-bound APC/C during the course of MG132 treatment. Nek2A will probably also bind apo-APC/C (compare Fig. 4E, APC4 immunoprecipitation versus BubR1 immunoprecipitation).

We conclude that the mechanisms by which cyclin A and Nek2A escape stabilization by the spindle checkpoint are most likely different, for the following reasons: (1) Nek2A starts to be degraded exactly at the prophase-to-prometaphase transition, which in most experiments, is detectable several min before cyclin A starts to decline – this difference might be explained by the special dependence of cyclin A destruction on competition between spindle checkpoint proteins and cyclin A for Cdc20 binding; (2) in contrast to that of cyclin A, Nek2A destruction is completely insensitive to increased MCC formation induced by nocodazole treatment; (3) Nek2A destruction, but not cyclin A destruction, proceeds effectively under conditions of ~95% Cdc20 depletion, or after 20 µM proTAME treatment; (4) although cyclin A degradation was found to depend on a competition mechanism between cyclin A and BubR1, required to liberate Cdc20 (Di Fiore and Pines, 2010), Nek2A, even at high concentrations, does not compete for BubR1 binding to Cdc20 *in vitro* (Sedgwick et al., 2013); indeed, here we show that Nek2A can form complexes with BubR1-inhibited APC/C; and (5) Nek2A bound to the APC/C in G2 phase, prior to its destruction in mitosis, whereas cyclin A, in complex with Cdc20, was only recruited to the APC/C from prometaphase onwards, when it is also degraded (Wolthuis et al., 2008).

Interestingly, in *in vitro* APC/C ubiquitylation assays, Cdc20 that is part of the MCC also has a small positive effect on APC/C activity (Herzog et al., 2009; Izawa and Pines, 2015; Kelly et al., 2014). In addition, autoubiquitylation of Cdc20 occurs while the checkpoint is actively inhibiting the APC/C, showing that the APC/C, in principle, can target its substrates regardless of being bound to the MCC (Foster and Morgan, 2012; Ma and Poon, 2011; Nilsson et al., 2008; Uzunova et al., 2012; Visconti et al., 2010). Taking observations together, we therefore propose that, in cells, binding of spindle checkpoint proteins does not completely prevent the ability of Cdc20 to activate the APC/C to the minimal level that is required to efficiently process Nek2A. APC/C^{MCC} (or APC/C$^{MCC\text{-}CDC20}$, see Izawa and Pines 2015) probably has a catalytic activity that is slightly higher than that of late prophase APC/C, when Emi1 is degraded but Cdc20 is not yet bound. This activity forms right at NEBD, by the binding of MCC to phosphorylated APC/C. Formation of APC/C^{MCC} alone does not lead to cyclin A turnover, but might just be sufficient to catalyze the Cdc20-dependent degradation of Nek2A, immediately at the prophase-to-prometaphase transition. Nevertheless, we cannot fully rule out that, in cells, a small amount of Cdc20 will never be incorporated into the MCC, but still binds to the APC/C at the start of mitosis and is responsible for Nek2A destruction.

Degradation of a Nek2A mutant that is not pre-recruited to the APC/C, Nek2AΔMR, requires spindle checkpoint release

Mutation of the TPR-binding MR tail of Nek2A prevents its binding to the APC/C, including in G2 phase (Fig. 5A), and delays, but does not prevent, Nek2A degradation in mitosis (Hayes et al., 2006; Sedgwick et al., 2013). Because we found that Nek2A destruction is entirely Cdc20 dependent, we reasoned that in the absence of APC/C binding by its MR tail, Nek2A should turn into a spindle-checkpoint-controlled substrate. To test this, we generated cell lines stably expressing a mutant of Venus–Nek2A lacking the MR tail (Venus–Nek2AΔMR) together with the spindle-checkpoint-target geminin–Cherry (Clijsters et al., 2013). When comparing these two substrates in single cells, we found a complete overlap of their destruction curves (Fig. 5B, note that here the graphs are synchronized around anaphase onset; supplementary material Fig. S1A). Importantly, degradation of Nek2AΔMR became highly sensitive to Cdc20 depletion, similar to that of geminin (Fig. 5C). We also compared the timing of Nek2AΔMR destruction to that of Aurora-A–eCFP, a known APC/C^{Cdh1} substrate (Floyd et al., 2008; Honda et al., 2000), and found that Venus–Nek2AΔMR was degraded well before Aurora A (supplementary material Fig. S4A) and independently of Cdh1 (supplementary material Fig. S4B). Nek2AΔMR remained largely stable during a taxol-induced mitotic delay (supplementary material Fig. S4C), similar to cyclin B1 (Brito and Rieder, 2006; Clute and Pines, 1999; Gascoigne and Taylor, 2008). When the spindle checkpoint was silenced by the Mps1 inhibitor reversine, destruction of geminin–Venus and Cherry–Nek2AΔMR began at NEBD (Fig. 5D). We conclude that abolishing the binding of Nek2A to the APC/C makes Nek2A destruction strictly dependent on an activity of Cdc20 that can only be released by passing the spindle checkpoint.

Journal of Cell Science (2015) 128, 1639–1653 doi:10.1242/jcs.163279

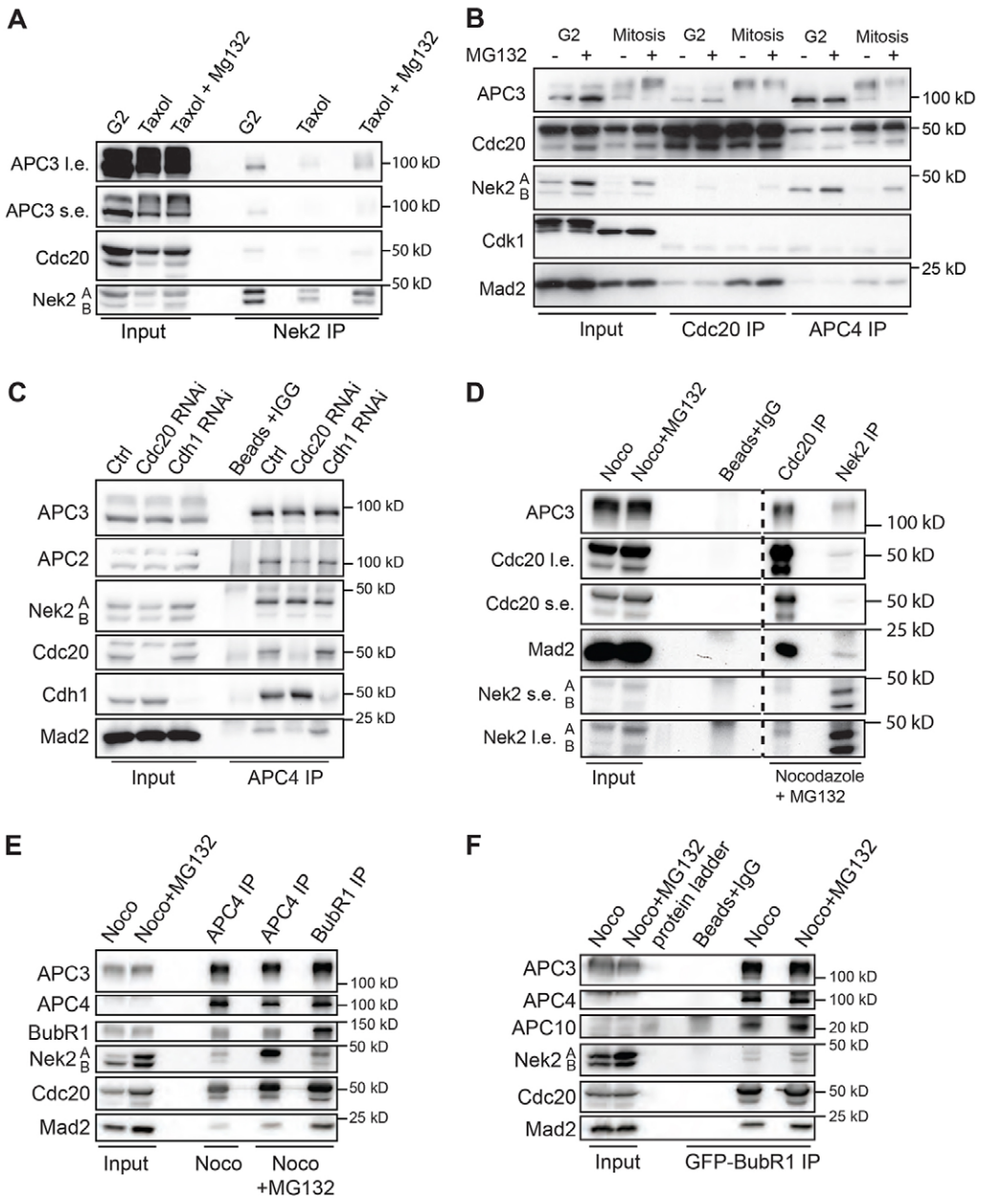

Fig. 4. Nek2A is recruited to the APC/C in G2-phase as well as in mitosis, independently of Cdc20. (A) To compare binding of Nek2A to the APC/C in G2-phase versus in mitosis, we compared U2OS cells released from an 8-h thymidine block (G2) to cells released from a 24-h thymidine block into taxol for 16 h (Taxol) and after 2 h addition of MG132 (Taxol+Mg132). Nek2 antibodies were used for precipitation (Nek2 IP), followed by western blot analysis. APC3 l.e., long exposure; APC3 s.e., short exposure. (B) Immunoprecipitations were performed on lysates from cells released from an 8-h thymidine-block in G2-phase, and cells synchronized by thymidine and released into nocodazole from which mitotic cells were collected by 'shake off' (Mitosis). Proteasome inhibitor MG132 was added where indicated, to reveal unstable protein. Lysates were equally divided for precipitations with antibodies as indicated. (C) U2OS cells were transfected with the indicated siRNA (RNAi) and synchronized in G2-phase by thymidine treatment followed by 8 h release. APC4 antibodies were used to immunoprecipitate the APC/C. Ctrl, control cells; Beads+IGG, IgG only control. (D) Cells were synchronized by thymidine and release into nocodazole (Noco), and treated for the final 2 h with proteasome inhibitor when indicated (Noco+MG132). Lysate was divided and Cdc20 and Nek2 were precipitated with antibodies. Take note that the Nek2 antibody recognizes and precipitates both the Nek2A and Nek2B isoform. Nek2 l.e., long exposure; Nek2 s.e., short exposure. (E) U2OS cells were synchronized as in D, and lysate from mitotic cells treated for 2 h with proteasome inhibitor were divided to precipitate either APC4 or BubR1. (F) HeLa cells expressing LAP–BubR1 were synchronized as in D, and anti-GFP antibodies were used to precipitate the ectopically expressed BubR1.

A Nek2A mutant that lacks the APC/C recruitment tail and the KEN destruction motif is stable in mitosis

The model emerging from our study is that spindle-checkpoint-restricted APC/C^{Cdc20} has sufficient catalytic activity to initiate destruction of Nek2A, provided that Nek2A is constitutively recruited towards the APC/C. Spindle checkpoint proteins typically prevent the binding of Cdc20 to a destruction motif such as the D-box or the KEN box. The Nek2 gene is spliced into three different isoforms of which Nek2A is the longest (Wu et al., 2007). This is the only isoform to contain an evolutionary conserved KEN box. In line with the spindle-checkpoint independence of Nek2A destruction, mutating the KEN box did

Journal of Cell Science (2015) 128, 1639–1653 doi:10.1242/jcs.163279

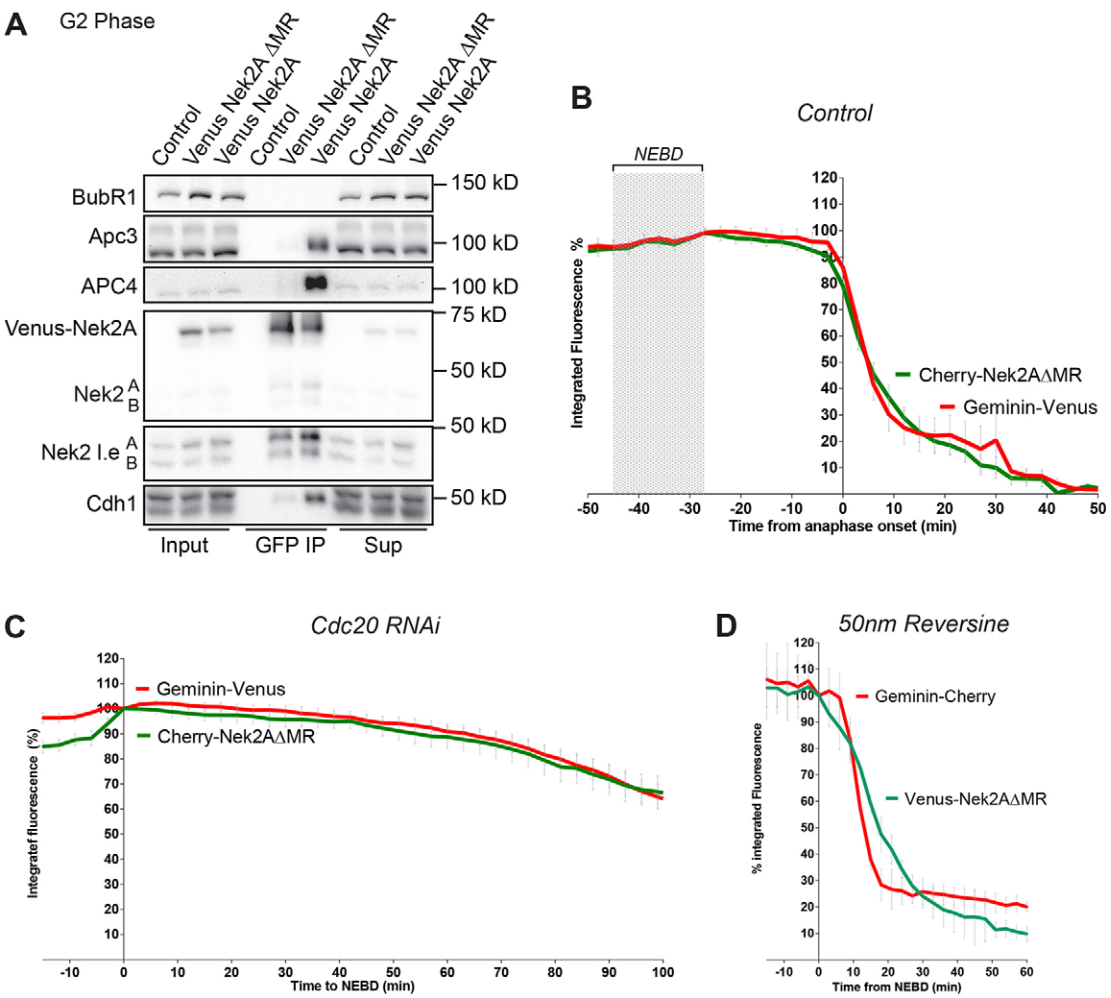

Fig. 5. Degradation of a Nek2A mutant that is not recruited to the APC/C, Nek2AΔMR, is delayed until spindle checkpoint release. (A) U2OS cells stably expressing Venus–Nek2A or Venus–Nek2AΔMR were synchronized in G2 by an 8 h release from thymidine block. Nek2A fusion protein was precipitated with anti-GFP nano-trap beads (GFP IP) after lysis. The supernatant (Sup) shows protein not bound to antibody-coupled beads. (B) U2OS cells stably transduced with Venus–Nek2AΔMR and geminin–Cherry constructs were imaged by fluorescence and DIC microscopy at 3-min intervals. In this case, the degradation curves were synchronized by the onset of sister chromatid separation at the start of anaphase, as judged by DIC. Results are mean±s.e.m. (n=10). (C) U2OS cells stably transduced with Venus–Nek2AΔMR and geminin–Cherry constructs were treated with Cdc20 siRNA (RNAi) and cells with mitotic delay were quantified for fluorescence levels (mean time from NEBD to anaphase is 113.5 min). Results are mean±s.e.m. (n=17 from the independent experiments). (D) U2OS cells stably transduced with Venus–Nek2AΔMR and geminin–Cherry were imaged by fluorescence and DIC microscopy at 3-min intervals, in the presence of 50 nm reversine. Levels were normalized to the frame when NEBD started. Results are mean±s.d. (n=5).

not stabilize Nek2A (Cherry–Nek2A-AEN, Fig. 6A; supplementary material Fig. S1A; also see Sedgwick et al., 2013). Then, we investigated whether the KEN box could contribute to the spindle-checkpoint-dependent destruction of Nek2AΔMR. Interestingly, a double Nek2A mutant, lacking both the APC/C-binding tail and the KEN destruction motif, remained fully stable throughout mitosis (Fig. 6B; supplementary material Fig. S1A). First, this result confirms that Nek2A degradation is indeed entirely dependent on the APC/C. Second, it shows that the spindle checkpoint very effectively blocks the recognition of the Nek2A KEN box by APC/C^{Cdc20}. Normally, this does not already occur in mitosis because Nek2A has largely disappeared when cells reach anaphase. The Nek2A KEN box did not play a role in binding Nek2A to the APC/C in G2 phase (Fig. 6C). These results imply that preventing binding of destruction motifs, like the KEN box, to Cdc20 is the main mechanism by which the spindle checkpoint stabilizes APC/C substrates in prometaphase. Indeed, the MCC complex inhibits APC/C^{Cdc20} by binding to the KEN box and D-box receptor (Izawa and Pines, 2015). Nek2A destruction normally does not depend on a destruction motif, so it can start in the presence of an active spindle checkpoint as soon as Cdc20 activates the APC/C. Only after satisfaction of the spindle checkpoint, does APC/C^{Cdc20} start to recognize APC/C destruction motifs such as the cyclin B1 D-box, or the Nek2A KEN box.

Removal of the spindle checkpoint accelerates Nek2A degradation

Although the spindle checkpoint inhibits the binding of Cdc20 to destruction motifs (Chao et al., 2012), it is possible that the checkpoint also impairs, at least to some extent, the ability of Cdc20 to promote the catalytic activity of the APC/C (Izawa and Pines, 2012). Indeed, *in vitro* APC/C^{MCC}, although not completely inactive, is less active than checkpoint-free APC/C^{Cdc20} (Fang, 2002; Herzog et al., 2009; Tang et al., 2001). This

Journal of Cell Science (2015) 128, 1639–1653 doi:10.1242/jcs.163279

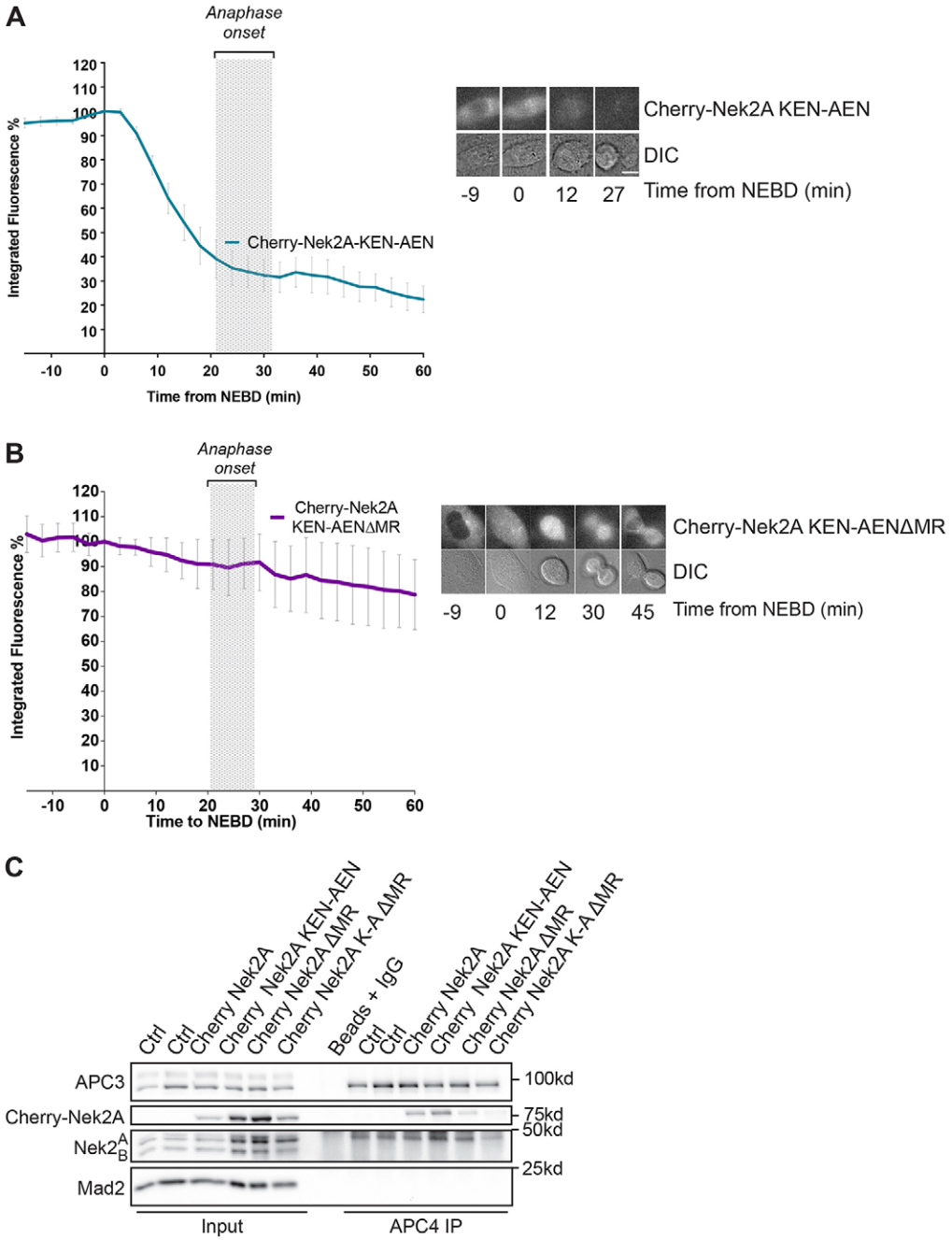

Fig. 6. A Nek2A double mutant lacking its APC/C pre-recruitment tail as well as its spindle-checkpoint-controlled Cdc20-binding box (KEN) is fully stable in mitosis. (A) U2OS cells stably transduced with Cherry–Nek2A-KEN-AEN were imaged by fluorescence and DIC microscopy. Integrated fluorescence was measured and normalized to 100% at the start of NEBD as described in the legend to Fig. 1. Scale bar: 10 μm. (B) U2OS cells stably transduced with Cherry–Nek2A-KEN-AENΔMR were imaged by fluorescence and time lapse microscopy as in A. (C) U2OS cells stably expressing Cherry–Nek2A or its mutant versions were synchronized in G2 by 8 h release after 24 h thymidine treatment. After lysis the APC/C was immunoprecipitated (IP) using APC4 antibodies and analyzed by western blotting. Ctrl, control cells; Beads+IgG, IgG only control.

is in line with several other studies showing that the checkpoint inhibits APC/C catalytic activity (Maciejowski et al., 2010; Mansfeld et al., 2011; Sliedrecht et al., 2010).

Next, we tested whether inability to activate the spindle checkpoint at the prophase-to-prometaphase transition would further increase APC/C^{Cdc20} activity towards Nek2A, as also shown for cyclin A (Collin et al., 2013). Therefore, we abolished the spindle checkpoint by treating G2 phase cells with the Mps1 inhibitor reversine (Kwiatkowski et al., 2010; Schmidt et al., 2005) or with Mad2 siRNA, and measured the degradation of geminin–Cherry and Venus–Nek2A as cells entered mitosis (Fig. 7A, upper panel and lower panel, respectively). The average time from NEBD to anaphase in control cells was 25.4 min (±4.8 s.d.) (Fig. 7B,C), whereas bypass of the checkpoint reduced the duration of mitosis to 14.3 min (±2.5 s.d.; reversine) and 12.6 min (±1.9 s.d.; Mad2-RNAi) (Fig. 7B,C). Geminin–Cherry levels reached 50% of their maximal fluorescence within 31.3 min in controls (±8.1 s.d.), which was accelerated approximately twofold by either of the two means of checkpoint inhibition, to 15.8 min (±2.1 s.d.) in reversine-treated cells and 15.4 min (±3.0 s.d.) for Mad2 siRNA cells (Fig. 7B,C). Remarkably, Nek2A was also degraded approximately twofold faster after silencing the spindle checkpoint: we found a decrease in half-life from 14.36 min in controls to 8.0 min (±1.5 s.d.) for reversine-treated cells and 8.7 min (±1.8 s.d.) for Mad2-depleted cells (Fig. 7A–C). Under both experimental conditions, the order of substrate degradation was unaltered, which is in line with the idea that direct Nek2A binding to the APC/C makes it a uniquely

Journal of Cell Science (2015) 128, 1639–1653 doi:10.1242/jcs.163279

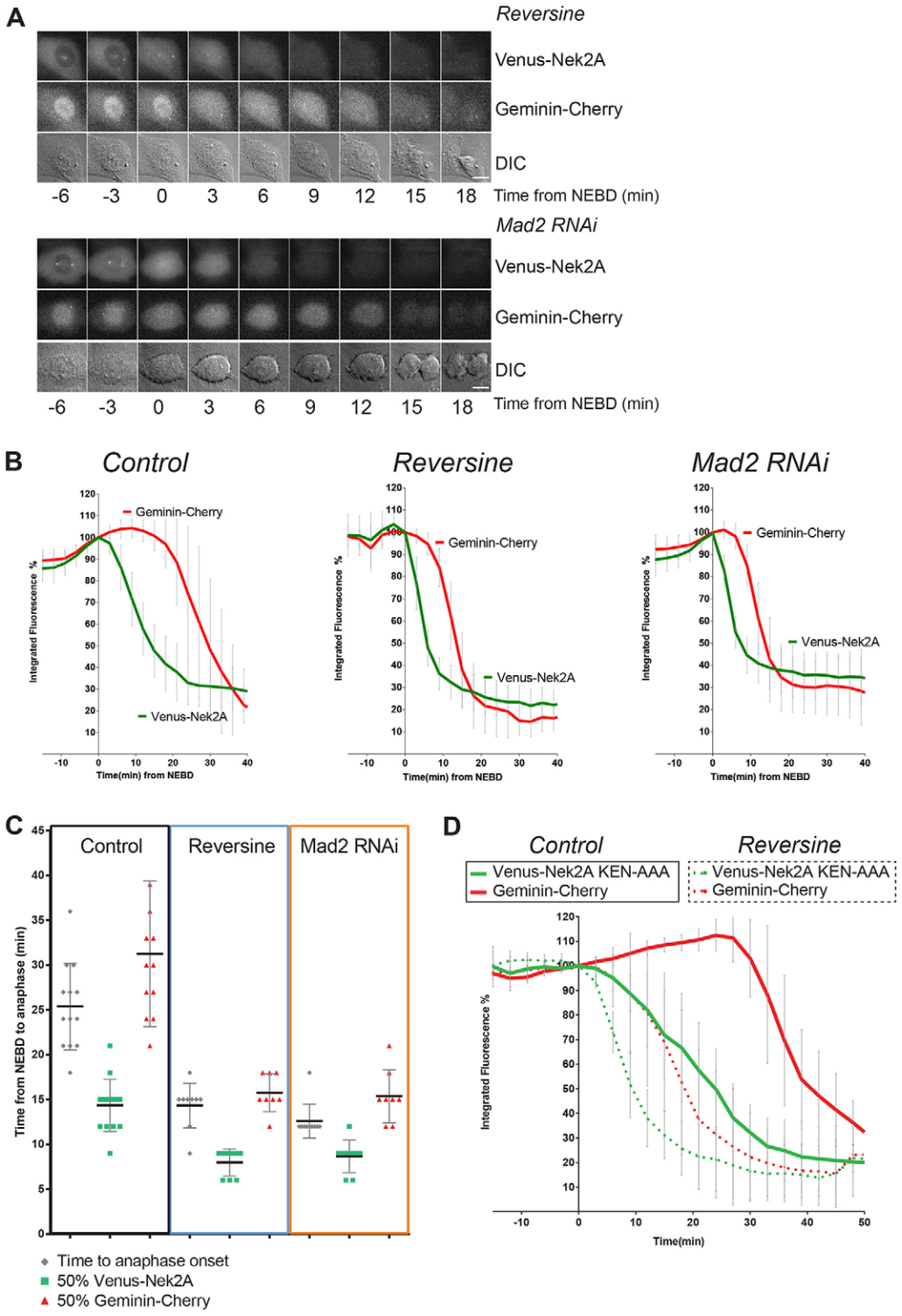

Fig. 7. Checkpoint silencing accelerates Nek2A destruction independently of the Nek2A KEN box but does not alter the order of substrate processing. (A) Panels of U2OS cells stably transduced with geminin–Cherry and Venus–Nek2A were imaged by fluorescent and DIC microscopy. The spindle checkpoint was abrogated by treatment with 50 nm reversine (upper panesl) or by depletion of Mad2 by siRNA (RNAi) (lower panels) Scale bars: 10 μm. (B) Graphs represent the mean±s.d. integrated fluorescence intensity, normalized to 100% fluorescence at frame of NEBD as indicated in the legend of Fig. 1. Control cells, $n=10$; reversine, $n=10$; Mad2 RNAi, $n=10$. (C) From the time-lapse experiments shown in B, the time from NEBD to anaphase as judged by fluorescent and DIC channel as well as the time to 50% fluorescence is plotted for Venus–Nek2A and geminin–Cherry in normal mitosis, or reversine-treated and Mad2-depleted mitotic cells. The mean±s.d. is also shown. (D) Cells expressing stably expressing Venus–Nek2A-KEN-AAA were imaged at 3-min intervals as described in the legend to Fig. 1, in either the control situation (solid line) or in the presence of 50 nm reversine (dotted line).

effective substrate. We then investigated whether the KEN box played a crucial role in accelerating degradation of Nek2A in the absence of the spindle checkpoint. Although a single point mutant in the KEN box was enough to prevent binding in the absence of the MR tail (Fig. 6C), we now mutated the complete KEN box. Importantly, the destruction of a complete alanine-substitution mutant of the Nek2A KEN box, Venus–Nek2A-KEN-AAA, also occurred faster upon reversine treatment (Fig. 7D). Taken together, these results therefore indicate that removal of the spindle checkpoint, independently from facilitating the recognition of a KEN box by Cdc20, slightly increases APC/C^{Cdc20} activity from the start of prometaphase onwards. In conclusion, the spindle checkpoint predominantly blocks binding of Cdc20 to destruction motifs in APC/C substrates, but also slightly attenuates the catalytic activity of APC/C^{Cdc20} in prometaphase. The latter inhibitory effect of the spindle

Journal of Cell Science (2015) 128, 1639–1653 doi:10.1242/jcs.163279

checkpoint is insufficient to prevent Nek2A destruction and is also not enforced by spindle poisons.

DISCUSSION

Different pathways direct the spindle-checkpoint-independent destruction of Nek2A and cyclin A

The stability of every APC/C substrate might be governed in a unique way to ensure its degradation occurs at a specific point in the cell cycle (e.g. Lu et al., 2014). Cyclin A and cyclin B1 are both APC/C substrates that similarly depend on Cdc20 for their destruction, but they are degraded at different times in mitosis (Wolthuis et al., 2008). Whereas cyclin A gets degraded in prometaphase, cyclin B1 is stabilized by the spindle checkpoint until metaphase. Previously, we and others have shown that the N-terminus of cyclin A binds to Cdc20 in such a way that it competitively inhibits the ability of checkpoint proteins to bind Cdc20. These 'checkpoint-free' cyclin-A–Cdc20 complexes are then recruited to the phosphorylated APC/C in mitosis (Fig. 8). Here, we show that another mitotic regulator that disappears rapidly in prometaphase, Nek2A, requires only very limited amounts of Cdc20 to be degraded effectively. Nek2A destruction also does not detectably depend on binding to Cdc20, or on a canonical KEN box or D-box destruction motif. Inhibiting the ability of APC/C^{Cdc20} to bind to destruction boxes, by treatment with the recently discovered APC/C inhibitor APCin, did not stabilize Nek2A [Sackton et al., 2014; and unpublished data]. Nevertheless, Nek2A relies exclusively on APC/C^{Cdc20} to be degraded in mitosis: simultaneously reducing Cdc20 levels by siRNA, combined with inhibiting Cdc20 binding to the APC/C by proTAME, completely blocks Nek2A destruction. Reducing the levels of APC/C subunits by siRNA had surprisingly little effect on Nek2A degradation, especially when compared to spindle-checkpoint-dependent APC/C^{Cdc20} substrates. This most likely reflects the fact that Nek2A is a very effective APC/C substrate: Nek2A is constantly targeted to the APC/C, possibly to the TPR motif containing APC8 [although a role for other subunits has not been excluded (see also, Sedgwick et al., 2013)], and this renders Nek2A highly sensitive for efficient Cdc20-dependent degradation.

By treating mitotic cells with nocodazole, more checkpoint signal is generated, as Mad2 is bound threefold as effectively to Cdc20 (Collin et al., 2013). This slows down cyclin A

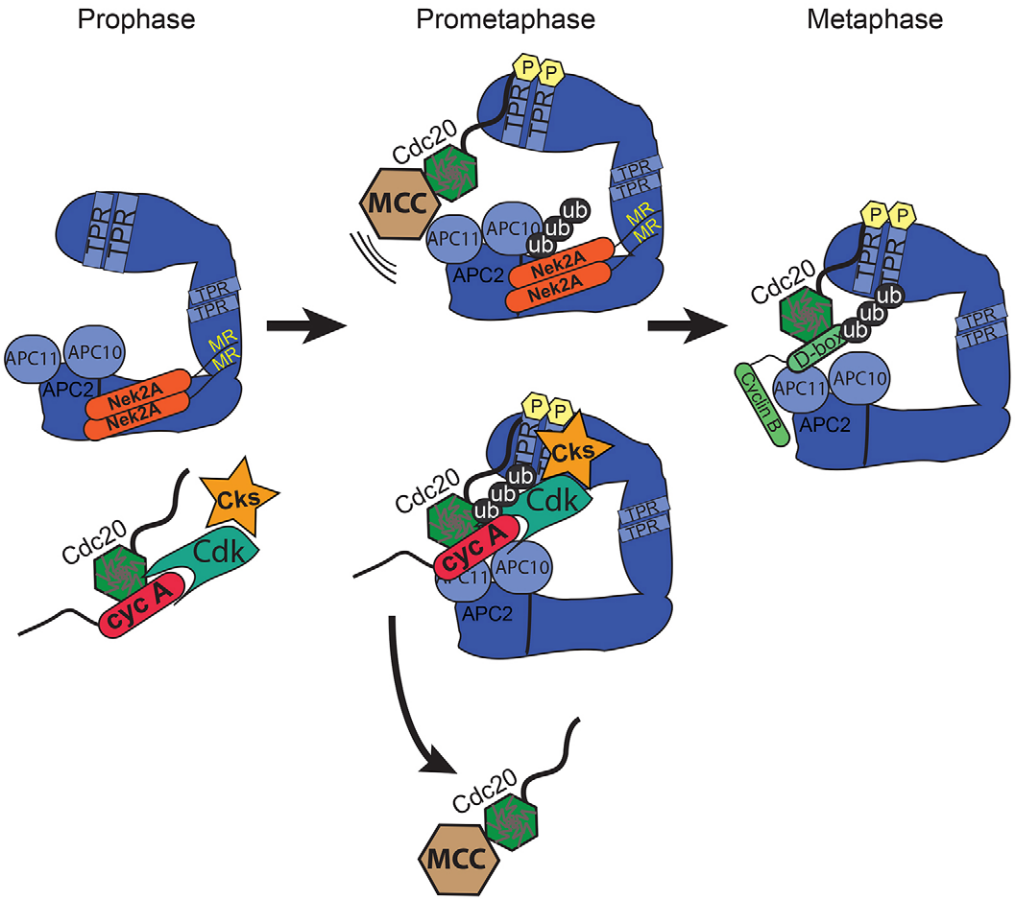

Fig. 8. Cdc20-independent binding of Nek2A in G2 and activation of the APC/C by Cdc20 direct the destruction of Nek2A in the spindle checkpoint. In prophase, the APC/C inhibitor Emi1 is degraded and Cdh1 is removed from the APC/C (e.g. by increasing Cdk1-dependent phosphorylation). Therefore, at this time in the cell cycle, the APC/C is mostly present as a complex without co-activator bound. TPR, TPR motif in the APC/C; MR, MR motifs in Nek2A. At mitotic entry, Cdc20 starts to bind the APC/C and the spindle checkpoint is activated. Nek2A binding to the APC/C is not regulated by mitotic entry or the presence of a co-activator (represented by prometaphase). Upon transition to mitosis (represented by metaphase), Cdc20 activates the APC/C, whether or not it is restricted by the mitotic checkpoint (MCC) and this allows for immediate degradation of pre-recruited Nek2A, in a manner independent of a known Cdc20-binding destruction motif or of significant amounts of Cdc20. We observe no competition between Cdc20 and Nek2A for APC/C binding nor an increase in Nek2A binding to the APC/C when cells enter mitosis. We propose that this reflects the catalytic activation of the APC/C by induced binding of Cdc20. Geminin and cyclin B1 bind the APC/C in a D-box and Cdc20-dependent manner and is processed in metaphase. P, phosphorylation; ub, ubiquitylation.

degradation but not Nek2A degradation. An attenuating effect of increasing spindle checkpoint strength on cyclin A disappearance fits with the unique requirement for competition between cyclin A and spindle checkpoint proteins for Cdc20 binding.

The time when Nek2A destruction begins in mitosis is not set by increased Nek2A recruitment to Cdc20 or the APC/C, but marks the point when Cdc20 starts to catalytically activate the APC/C (Fig. 8). In contrast, cyclin A destruction requires the prior formation of stable complexes between cyclin A and Cdc20, their timely recruitment to the prometaphase APC/C, and finally a function of Cdc20 that is sensitive to the spindle checkpoint, possibly the positioning of the cyclin A N-terminus towards the active site of the APC/C (Fig. 8).

Nek2A disappearance marks the point when Cdc20, regardless of the spindle checkpoint, activates the APC/C

Although we recently discovered that Nek2A is very slowly degraded by an APC/C-dependent mechanism during S and G2 phases (Hames et al., 2005; and our unpublished data), Nek2A disappears only in mitosis. This not due to decreased translation of Nek2A at mitotic entry, because Nek2A is still rapidly synthesized in mitosis (e.g. see Fig. 4B). We think that the simplest model explaining our data is that rapid Nek2A disappearance marks the point when Cdc20, regardless of its incorporation into or inhibition by the MCC, activates the APC/C at the prophase-to-prometaphase transition.

At mitotic entry, Cdc20 binds the APC/C by means of its C-terminal tail (Vodermaier et al., 2003), the KILR motif (Izawa and Pines, 2012) and by its N-terminal C-box (Kimata et al., 2008). The binding of Cdc20 to the APC/C is enforced by mitotic phosphorylation of the APC/C, but also by the spindle checkpoint: the Cdc20 C-box might be involved in stabilizing complexes between the APC/C and spindle checkpoint proteins (Hein and Nilsson, 2014). Hence, Cdc20, when incorporated in the MCC, effectively forms complexes with the APC/C at the start of prometaphase. Recent *in vitro* data showed that Nek2A ubiquitylation might be refractory to increasing levels of checkpoint proteins (Kelly et al., 2014). Moreover, activation of the E2 enzyme Ube2S does not seem to be hindered by the checkpoint proteins in its ability to elongate Nek2A monoubiquitin chains *in vitro* (Kelly et al., 2014). Intriguingly, the MCC has been shown to bind two Cdc20 molecules (Izawa and Pines, 2015), as has been hypothesized previously (Primorac and Musacchio, 2013). BubR1 blocks the substrate recognition domain of the Cdc20 molecule bound to the APC/C (Kraft et al., 2005; Lara-Gonzalez et al., 2011). We also find that the spindle checkpoint predominantly acts to prevent Cdc20 from binding to destruction motifs (Figs 5, 6). Nek2A destruction is only dependent on an APC/C-activating step that coincides with the association of Cdc20 to the APC/C in mitosis. However, a mutant of Nek2A, Nek2AΔMR, strictly needs a KEN box for its destruction and is easily stabilized by Cdc20 depletion, as well as being strictly controlled by the spindle checkpoint. This fits with the concept that the spindle checkpoint particularly blocks stoichiometric complex formation between Cdc20 and APC/C substrate destruction motifs.

Virtually no BubR1-free APC/C^{Cdc20} is detected in spindle-poison-arrested cells, unless these cells are treated with proteasome inhibitor (Herzog et al., 2009). This indicates that any Cdc20 free of checkpoint proteins is rapidly degraded in nocodazole-arrested cells (e.g. see Fig. 4E). This, combined with the observation that enforcing the spindle checkpoint does not delay Nek2A degradation, supports our hypothesis that even spindle-checkpoint-inhibited Cdc20 is able to partially activate the APC/C at prometaphase (Fig. 8). Alternatively, however, a very small fraction of APC/C^{Cdc20} could remain completely uninhibited during prometaphase and be sufficient for Nek2A destruction to proceed entirely regardless of the spindle checkpoint.

Role for spindle checkpoint silencing in further activating the APC/C after metaphase?

Our results reveal a paradoxical role of the spindle checkpoint in Nek2A degradation. Drug-induced enforcement of the spindle checkpoint cannot delay the time when Nek2A degradation starts but ablating the spindle checkpoint, by treating cells with Mps1 inhibitor or depleting Mad2, increases the rate by which Nek2A disappears. This can be explained by assuming that, whereas the spindle checkpoint blocks recognition of destruction motifs very effectively, it only moderately impairs the catalytic activity of the APC/C^{Cdc20} during prometaphase.

Interestingly, this would also imply that, in cells that pass through mitosis normally, APC/C^{Cdc20} gains further activity after spindle checkpoint release during metaphase and anaphase (Lindon and Pines, 2004). The nature of the increased APC/C^{Cdc20} activity could be twofold: either the C-box of Cdc20 becomes unrestricted by checkpoint release and triggers a catalytic activation of the APC/C complex to which it is already bound, or the total number of APC/C^{Cdc20} complexes in cells increases at metaphase, because the spindle checkpoint prevents accumulation of Cdc20 onto the APC/C in prometaphase (Mansfeld et al., 2011; Nilsson et al., 2008; Uzunova et al., 2012). While we were preparing this manuscript, the Barford laboratory published that binding of the N-terminal part of Cdh1 containing the C box, which is identical to the C box in Cdc20, is responsible for interaction with APC1 (Chang et al., 2014), and allows for conformational change of the APC/C catalytic module, APC2–APC11. Their work also implies that release of the spindle checkpoint enhances binding of ubiquitin-bound UbcH10, boosting the activity of the APC/C. Likely, checkpoint silencing will not only permit increased UbcH10 binding, but also increased Ube2S binding and thus higher APC/C catalytic activity (Van Voorhis and Morgan, 2014). Recently, we and others proposed that enhanced APC/C^{Cdc20} activity upon spindle checkpoint release might help to avoid the 'anaphase problem': the risk that separating sister chromatids when losing tension could re-impose the spindle checkpoint in case cyclin B1 is not completely degraded when cells reach anaphase (Clijsters et al., 2014; Kamenz and Hauf, 2014; Rattani et al., 2014; Vázquez-Novelle et al., 2014). The implications of these findings require further analysis of the way changes in APC/C^{Cdc20} influence mitotic exit.

MATERIALS AND METHODS

Tissue culture and cell cycle synchronization

Human osteosarcoma cells were grown in Dulbecco's modified Eagle's medium (DMEM; Gibco) containing FCS (Sigma), penicillin, streptomycin and cultured at 37℃ in 5% CO_2. At 24 or 48 h before synchronization or transfection, cells were plated on 9-cm Falcon dishes or, for time-lapse fluorescence microscopy on 3.5-mm glass-bottomed dishes (Wilco Wells) or four-well glass-bottomed dishes (Labtek II). For enrichment of cells in G2 phase, cells were treated for 24 h with thymidine (Sigma, 2,5 mM final concentration) and incubated for 8 h after release.

Other drugs, used as indicated, were: Mps1 inhibitor reversine (catalog number 10004412, 50 nM final concentration; Cayman Chemicals);

proteasome inhibitor MG132 (catalog number 13697, 5 µM final concentration; Cayman Chemicals); translation inhibitor cycloheximide (catalog number C6255, 5 or 10 µM final concentration; Sigma-Aldrich), RO-3306 (catalog number 217699, 3 µM final concentration; Calbiochem), ProTAME (I-440, 12 µM final concentration or as noted; R&D systems).

Plasmids

Nek2A was cloned from cDNA into a Clontech C1 vector, encoding either a Cherry or Venus fluophore, and subsequently cloned into Clontech pLib vectors. To create stable cell lines, Phoenix-ecotropic cell lines were transfected in six-well plates with 4 µg of pLIB-vector containing the insert of choice, using standard calcium phosphate transfection. Viral supernatant was collected three times, 40, 48 and 64 h after transfection. The supernatant was cleared through a 0.45-µm filter (EMD Millipore). U2OS cells expressing the ecotropic receptor (from Johan Kuiken, NKI, Amsterdam, Netherlands) were infected twice in the presence of polybrene.

Transfections and retroviral infection

Cells were transfected with 40 nM siRNA oligonucleotide pools (ON-TARGET-plus oligonucleotides, Dharmacon) using Lipofectamine 2000 (Invitrogen) according to the manufacturer's protocol. siRNAs (Thermo Fisher Scientific as ON-TARGET plus SMART pools) used were against: Nek2 (targeting both Nek2A and Nek2B), 5′-GGAUCUGGCUAGUGUAAUU-3′, 5′-GCAGACAGAUCCUGGGCAU-3′, 5′- GGCAAUACUUAGAUGAAGA-3′ and 5′- GCUAGAAUAUUAAACCAUG-3′; Cdc20 (CDC20), 5′-CGGAAGACCUGCCGUUACA-3′, 5′-GGGCCGAACUCCUGGCAAA-3′, 5′-GAUCAAAGAGGGCAACUAC-3′ and 5′-CAGAACAGACUGAAAGUAC-3′; Mad2 (MAD2L1), 5′-UUACUCGAGUGCAGAAAUA-3′, 5′-CUACUGAUCUUGAGCUCAU-3′, 5′-GGUUGUAGUUAUCUCAAAU-3′ and 5′-GAAAUCCGUUCAGUGAUCA-3′; Cdh1 (FZR), 5′-CCACAGGAUUAACGAGAAU-3′, 5′-GGAACACGCUGACAGGACA-3′, 5′-GCAACGAUGUGUCUCCCUA-3′ and 5′-GAAGAAGGGUCUGUUCACG-3′; APC2 (ANAPC2), 5′-GAGAUGAUCCAGCGUCUGU-3′, 5′-GACAUCAUCACCCUCUAUA-3′, 5′-GAUCGUAUCUACAACAUGC-3′ and 5′-GAGAAGAAGUCCACACUAU-3′; Apc10 (ANAPC10), 5′-GAGCUCCAUUGGUAAAUUU-3′, 5′-GAAAUUGGGUCACAAGCUG-3′, 5′-GCAAUCAGAUGGUUCCCAG-3′ and 5′-CAUGAUGUAUCGUUCAAUA-3′; APC3 (Cdc27), 5′-GGAAAUAGCCGAGAGGUAA-3′, 5′-CAAAAGAGCCUUAGUUUAA-3′, 5′-AAUGAUAGCCUGGAAAUUA-3′ and 5′-GCAUAUAGACUCUUGAAAG-3′; Ube2S (UBE2S), 5′-ACAAGGAGGUGACGACACU-3′, 5′-GGAGGUCUGUUCCGCAUGA-3′, 5′-GCAUCAAGGUCUUUCCCAA-3′ and 5′-CCAAGAAGCAUGCUGGCGA-3′; UbcH10 (Ube2C) 5′-GAACCCAACAUUGAUAGUC-3′, 5′-UAAAUUAAGCCUCGGUUGA-3′, 5′-GUAUAGGACUCUUUAUCUU-3′ and 5′-GCAAGAAACCUACUCAAAG-3′.

Antibodies

Antibodies used were: goat anti-actin (SC-1616, Santa Cruz Biotechnology), rabbit anti-APC2 (provided by Jonathon Pines, Department of Zoology, Gurdon Institute, Cambridge, UK), mouse anti-APC3 (BD Transduction), goat anti-APC4 (SC21414, Santa Cruz Biotechnology), goat anti-Cdc16/APC6 (1:1000; SC-6395, Santa Cruz Biotechnology), rabbit anti-APC10 (611501/2, Biolegend), mouse anti-BubR1 (Chemicon MAB3612; 1:500), rabbit anti-BubR1 (A300-386a, Bethyl), mouse anti-Cdc20/p55 (sc-13162, Santa Cruz Biotechnology), mouse anti-Nek2 (1:500; BD 610593), mouse anti-Cdk1 (Cell Signaling), mouse anti-Mad2 (MBL K0167-3), mouse anti-Cdh1 (MS1116-p1, Neomarkers), goat anti-Cdk4 (sc-260, Santa Cruz Biotechnology), rabbit anti-cyclin A2 (H-432, Santa Cruz Biotechnology), rabbit anti-TopoIIα (A300-054A-1, Bethyl), rabbit anti-PTTG-1/Securin (1:500; 34-1500, Zymed) and custom rabbit anti-GFP '2C' antibodies.

Western blotting and immunoprecipitations

Cells were lysed in ELB+ (150 mM NaCl, 50 mM HEPES pH 7.5, 5 mM EDTA, 0.3% NP-40, 10 mM β-glycerophosphate, 6% glycerol, 5 mM NaF, 1 mM Na_3VO_4 and Roche protease inhibitor cocktail). Lysates were cleared by centrifugation (13,000 ***g***, 12 min at 4℃). Protein levels were equalized by using Bradford analysis. For immunoprecipitations, 2 µg antibodies were precoupled for 4–12 h to 20 µl of protein-G–Sepharose (Amersham Biosciences) and washed with ELB+. Precoupled beads and lysates were incubated overnight at 4℃ and washed three times with 1.0 ml of ice-cold ELB+. All remaining buffer was removed and beads were resuspended in 60 µl sample buffer; 25 µl was separated by SDS-PAGE and blotted on nitrocellulose (0.4 µm pore). Immunoprecipitations of GFP were performed with GFP–Trap_A beads (Chromotek), according to the manufacturer's protocol. Membranes were blocked with 4% milk solution made from ELK powder (Campina Friesland, Amersfoort, The Netherlands) in PBS containing 0.1% Tween. Development of blots was achieved with either with silver film and scanning, or by using the Chemidoc Imaging System (Bio-Rad Laboratories) and quantification was performed with the Image Lab (Bio-Rad Laboratories) software.

Time-lapse fluorescence microscopy

U2OS or RPE1-TERT cells transfected with siRNA and the indicated plasmids were followed by fluorescence time-lapse microscopy. Acquisition of differential interference contrast (DIC) and fluorescence images started 24 or 48 h after transfection on a microscope (Axio Observer Z1; Carl Zeiss) in a heated culture chamber (5% CO_2 at 37℃) using DMEM with 8% FCS and antibiotics. The microscope was equipped with an LD 0.55 condenser and 40× NA 1.40 Plan Apochromat oil DIC objective and CFP/YFP and GFP/HcRed filter blocks (Carl Zeiss) to select specific fluorescence. Images were taken using AxioVision Rel. 4.8.1 software (Carl Zeiss) with a charge-coupled device camera [ORCA R2 Black and White CCD (Hamamatsu Photonics) or Roper HQ (Roper Scientific)] at 100-ms exposure times. Alternatively imaging was performed on a Deltavision Elite system, using L15 Leibovits medium (Gibco), in a 37℃ culture chamber, without the need of supplying CO_2.

For quantitative analysis of degradation, MetaMorph software (Universal Imaging), ImageJ (National Insitute of Health) and Excel (Microsoft) were used. Captured images were processed using Photoshop and Illustrator software (Adobe).

Acknowledgements

We thank Daisuke Izawa and Jon Pines for providing the APC2 antibody, Arne Lindqvist for sharing the U2OS Tet inducible Cyclin A2-Venus cell line, the Hyman lab for the LAP-BubR1 HeLA celline and Katarzyna Kedziora for assistance with Image J macro writing. We thank Erik Voets and other division members for fruitful discussion and critically reading the manuscript.

Competing interests

The authors declare no competing or financial interests.

Author contributions

R.M.F.W. devised the project and designed experiments, M.B. designed and performed all experiments. M.B. wrote the initial draft of the paper, which was supervised and edited by R.M.F.W.

Funding

This project was supported by Human Frontiers Science Program [grant number RGP0053/2010 to M.B. and R.M.F.W.].

Supplementary material

Supplementary material available online at
http://jcs.biologists.org/lookup/suppl/doi:10.1242/jcs.163279/-/DC1

References

Bahe, S., Stierhof, Y.-D., Wilkinson, C. J., Leiss, F. and Nigg, E. A. (2005). Rootletin forms centriole-associated filaments and functions in centrosome cohesion. *J. Cell Biol.* **171**, 27-33.

Bahmanyar, S., Kaplan, D. D., Deluca, J. G., Giddings, T. H., Jr, O'Toole, E. T., Winey, M., Salmon, E. D., Casey, P. J., Nelson, W. J. and Barth, A. I. M. (2008). beta-Catenin is a Nek2 substrate involved in centrosome separation. *Genes Dev.* **22**, 91-105.

Brito, D. A. and Rieder, C. L. (2006). Mitotic checkpoint slippage in humans occurs via cyclin B destruction in the presence of an active checkpoint. *Curr. Biol.* **16**, 1194-1200.

Chang, L., Zhang, Z., Yang, J., McLaughlin, S. H. and Barford, D. (2014). Molecular architecture and mechanism of the anaphase-promoting complex. *Nature* **513**, 388-393.
Chao, W. C. H., Kulkarni, K., Zhang, Z., Kong, E. H. and Barford, D. (2012). Structure of the mitotic checkpoint complex. *Nature* **484**, 208-213.
Clijsters, L., Ogink, J. and Wolthuis, R. (2013). The spindle checkpoint, APC/C(Cdc20), and APC/C(Cdh1) play distinct roles in connecting mitosis to S phase. *J. Cell Biol.* **201**, 1013-1026.
Clijsters, L., van Zon, W., Riet, B. T., Voets, E., Boekhout, M., Ogink, J., Rumpf-Kienzl, C. and Wolthuis, R. M. (2014). Inefficient degradation of cyclin B1 re-activates the spindle checkpoint right after sister chromatid disjunction. *Cell Cycle* **13**, 2370-2378.
Clute, P. and Pines, J. (1999). Temporal and spatial control of cyclin B1 destruction in metaphase. *Nat. Cell Biol.* **1**, 82-87.
Collin, P., Nashchekina, O., Walker, R. and Pines, J. (2013). The spindle assembly checkpoint works like a rheostat rather than a toggle switch. *Nat. Cell Biol.* **15**, 1378-1385.
da Fonseca, P. C. A., Kong, E. H., Zhang, Z., Schreiber, A., Williams, M. A., Morris, E. P. and Barford, D. (2011). Structures of APC/CCdh1 with substrates identify Cdh1 and Apc10 as the D-box co-receptor. *Nature* **470**, 274-278.
den Elzen, N. and Pines, J. (2001). Cyclin A is destroyed in prometaphase and can delay chromosome alignment and anaphase. *J. Cell Biol.* **153**, 121-136.
Di Fiore, B. and Pines, J. (2010). How cyclin A destruction escapes the spindle assembly checkpoint. *J. Cell Biol.* **190**, 501-509.
Dube, P., Herzog, F., Gieffers, C., Sander, B., Riedel, D., Müller, S. A., Engel, A., Peters, J. M. and Stark, H. (2005). Localization of the coactivator Cdh1 and the cullin subunit Apc2 in a cryo-electron microscopy model of vertebrate APC/C. *Mol. Cell* **20**, 867-879.
Fang, G. (2002). Checkpoint protein BubR1 acts synergistically with Mad2 to inhibit anaphase-promoting complex. **13**, 755-766. *Mol. Biol. Cell*
Floyd, S., Pines, J. and Lindon, C. (2008). APC/C Cdh1 targets aurora kinase to control reorganization of the mitotic spindle at anaphase. *Curr. Biol.* **18**, 1649-1658.
Foley, E. A. and Kapoor, T. M. (2013). Microtubule attachment and spindle assembly checkpoint signalling at the kinetochore. *Nat. Rev. Mol. Cell Biol.* **14**, 25-37.
Foster, S. A. and Morgan, D. O. (2012). The APC/C subunit Mnd2/Apc15 promotes Cdc20 autoubiquitination and spindle assembly checkpoint inactivation. *Mol. Cell* **47**, 921-932.
Fry, A. M., Meraldi, P. and Nigg, E. A. (1998a). A centrosomal function for the human Nek2 protein kinase, a member of the NIMA family of cell cycle regulators. *EMBO J.* **17**, 470-481.
Fry, A. M., Mayor, T., Meraldi, P., Stierhof, Y. D., Tanaka, K. and Nigg, E. A. (1998b). C-Nap1, a novel centrosomal coiled-coil protein and candidate substrate of the cell cycle-regulated protein kinase Nek2. *J. Cell Biol.* **141**, 1563-1574.
Fry, A. M., Arnaud, L. and Nigg, E. A. (1999). Activity of the human centrosomal kinase, Nek2, depends on an unusual leucine zipper dimerization motif. *J. Biol. Chem.* **274**, 16304-16310.
Gascoigne, K. E. and Taylor, S. S. (2008). Cancer cells display profound intra- and interline variation following prolonged exposure to antimitotic drugs. *Cancer Cell* **14**, 111-122.
Geley, S., Kramer, E., Gieffers, C., Gannon, J., Peters, J. M. and Hunt, T. (2001). Anaphase-promoting complex/cyclosome-dependent proteolysis of human cyclin A starts at the beginning of mitosis and is not subject to the spindle assembly checkpoint. *J. Cell Biol.* **153**, 137-148.
Hagting, A., Elzen, N. d. e. n, Vodermaier, H., Waizenegger, I., Peters, J. and Pines, J. (2002). Human securin proteolysis is controlled by the spindle checkpoint and reveals when the APC/C switches from activation by Cdc20 to Cdh1. *J. Cell Biol.* **157**, 1125-1137.
Hames, R. S., Wattam, S. L., Yamano, H., Bacchieri, R. and Fry, A. M. (2001). APC/C-mediated destruction of the centrosomal kinase Nek2A occurs in early mitosis and depends upon a cyclin A-type D-box. *EMBO J.* **20**, 7117-7127.
Hames, R. S., Crookes, R. E., Straatman, K. R., Merdes, A., Hayes, M. J., Faragher, A. J. and Fry, A. M. (2005). Dynamic recruitment of Nek2 kinase to the centrosome involves microtubules, PCM-1, and localized proteasomal degradation. *Mol. Biol. Cell* **16**, 1711-1724.
Hayes, M., Kimata, Y., Wattam, S. and Lindon, C. (2006). Early mitotic degradation of Nek2A depends on Cdc20-independent interaction with the APC/C. *Nat. Cell Biol.* **8**, 607-614.
Hein, J. B. and Nilsson, J. (2014). Stable MCC binding to the APC/C is required for a functional spindle assembly checkpoint. *EMBO Rep.* **15**, 264-272.
Herzog, F., Primorac, I., Dube, P., Lenart, P., Sander, B., Mechtler, K., Stark, H. and Peters, J. (2009). Structure of the anaphase-promoting complex/cyclosome interacting with a mitotic checkpoint complex. *Science* **323**, 1477-1481.
Honda, K., Mihara, H., Kato, Y., Yamaguchi, A., Tanaka, H., Yasuda, H., Furukawa, K. and Urano, T. (2000). Degradation of human Aurora2 protein kinase by the anaphase-promoting complex-ubiquitin-proteasome pathway. *Oncogene* **19**, 2812-2819.
Izawa, D. and Pines, J. (2012). Mad2 and the APC/C compete for the same site on Cdc20 to ensure proper chromosome segregation. *J. Cell Biol.* **199**, 27-37.
Izawa, D. and Pines, J. (2015). The mitotic checkpoint complex binds a second CDC20 to inhibit active APC/C. *Nature* **517**, 631-634.
Kabeche, L. and Compton, D. A. (2013). Cyclin A regulates kinetochore microtubules to promote faithful chromosome segregation. *Nature* **502**, 110-113.
Kamenz, J. and Hauf, S. (2014). Slow checkpoint activation kinetics as a safety device in anaphase. *Curr. Biol.* **24**, 646-651.
Kelly, A., Wickliffe, K. E., Song, L., Fedrigo, I. and Rape, M. (2014). Ubiquitin chain elongation requires E3-dependent tracking of the emerging conjugate. *Mol. Cell* **56**, 232-245.
Kim, S. and Yu, H. (2011). Mutual regulation between the spindle checkpoint and APC/C. *Semin. Cell Dev. Biol.* **22**, 551-558.
Kimata, Y., Baxter, J. E., Fry, A. M. and Yamano, H. (2008). A role for the Fizzy/Cdc20 family of proteins in activation of the APC/C distinct from substrate recruitment. *Mol. Cell* **32**, 576-583.
Kraft, C., Vodermaier, H. C., Maurer-Stroh, S., Eisenhaber, F. and Peters, J.-M. (2005). The WD40 propeller domain of Cdh1 functions as a destruction box receptor for APC/C substrates. *Mol. Cell* **18**, 543-553.
Kramer, E. R., Scheuringer, N., Podtelejnikov, A. V., Mann, M. and Peters, J. M. (2000). Mitotic regulation of the APC activator proteins CDC20 and CDH1. *Mol. Biol. Cell* **11**, 1555-1569.
Kwiatkowski, N., Jelluma, N., Filippakopoulos, P., Soundararajan, M., Manak, M. S., Kwon, M., Choi, H. G., Sim, T., Deveraux, Q. L., Rottmann, S. et al. (2010). Small-molecule kinase inhibitors provide insight into Mps1 cell cycle function. *Nat. Chem. Biol.* **6**, 359-368.
Lara-Gonzalez, P., Scott, M. I. F., Diez, M., Sen, O. and Taylor, S. S. (2011). BubR1 blocks substrate recruitment to the APC/C in a KEN-box-dependent manner. *J. Cell Sci.* **124**, 4332-4345.
Lara-Gonzalez, P., Westhorpe, F. G. and Taylor, S. S. (2012). The spindle assembly checkpoint. *Curr. Biol.* **22**, R966-R980.
Lindon, C. and Pines, J. (2004). Ordered proteolysis in anaphase inactivates Plk1 to contribute to proper mitotic exit in human cells. *J. Cell Biol.* **164**, 233-241.
Lu, D., Hsiao, J. Y., Davey, N. E., Van Voorhis, V. A., Foster, S. A., Tang, C. and Morgan, D. O. (2014). Multiple mechanisms determine the order of APC/C substrate degradation in mitosis. *J. Cell Biol.* **207**, 23-39.
Ma, H. T. and Poon, R. Y. C. (2011). Orderly inactivation of the key checkpoint protein mitotic arrest deficient 2 (MAD2) during mitotic progression. *J. Biol. Chem.* **286**, 13052-13059.
Maciejowski, J., George, K. A., Terret, M. E., Zhang, C., Shokat, K. M. and Jallepalli, P. V. (2010). Mps1 directs the assembly of Cdc20 inhibitory complexes during interphase and mitosis to control M phase timing and spindle checkpoint signaling. *J. Cell Biol.* **190**, 89-100.
Mansfeld, J., Collin, P., Collins, M. O., Choudhary, J. S. and Pines, J. (2011). APC15 drives the turnover of MCC-CDC20 to make the spindle assembly checkpoint responsive to kinetochore attachment. *Nat. Cell Biol.* **13**, 1234-1243.
Mardin, B. R., Lange, C., Baxter, J. E., Hardy, T., Scholz, S. R., Fry, A. M. and Schiebel, E. (2010). Components of the Hippo pathway cooperate with Nek2 kinase to regulate centrosome disjunction. *Nat. Cell Biol.* **12**, 1166-1176.
Matyskiela, M. E. and Morgan, D. O. (2009). Analysis of activator-binding sites on the APC/C supports a cooperative substrate-binding mechanism. *Mol. Cell* **34**, 68-80.
Nilsson, J., Yekezare, M., Minshull, J. and Pines, J. (2008). The APC/C maintains the spindle assembly checkpoint by targeting Cdc20 for destruction. *Nat. Cell Biol.* **10**, 1411-1420.
Peters, J. M. (2006). The anaphase promoting complex/cyclosome: a machine designed to destroy. *Nat. Rev. Mol. Cell Biol.* **7**, 644-656.
Pines, J. (2011). Cubism and the cell cycle: the many faces of the APC/C. *Nat. Rev. Mol. Cell Biol.* **12**, 427-438.
Primorac, I. and Musacchio, A. (2013). Panta rhei: the APC/C at steady state. *J. Cell Biol.* **201**, 177-189.
Rattani, A., Vinod, P. K., Godwin, J., Tachibana-Konwalski, K., Wolna, M., Malumbres, M., Novák, B. and Nasmyth, K. (2014). Dependency of the spindle assembly checkpoint on Cdk1 renders the anaphase transition irreversible. *Curr. Biol.* **24**, 630-637.
Sackton, K. L., Dimova, N., Zeng, X., Tian, W., Zhang, M., Sackton, T. B., Meaders, J., Pfaff, K. L., Sigoillot, F., Yu, H., et al. (2014). Synergistic blockade of mitotic exit by two chemical inhibitors of the APC/C. *Nature* **514**, 646-649.
Schmidt, M., Budirahardja, Y., Klompmaker, R. and Medema, R. H. (2005). Ablation of the spindle assembly checkpoint by a compound targeting Mps1. *EMBO Rep.* **6**, 866-872.
Sedgwick, G. G., Hayward, D. G., Di Fiore, B., Pardo, M., Yu, L., Pines, J. and Nilsson, J. (2013). Mechanisms controlling the temporal degradation of Nek2A and Kif18A by the APC/C-Cdc20 complex. *EMBO J.* **32**, 303-314.
Skoufias, D. A., Indorato, R. L., Lacroix, F., Panopoulos, A. and Margolis, R. L. (2007). Mitosis persists in the absence of Cdk1 activity when proteolysis or protein phosphatase activity is suppressed. *J. Cell Biol.* **179**, 671-685.
Sliedrecht, T., Zhang, C., Shokat, K. M. and Kops, G. J. P. L. (2010). Chemical genetic inhibition of Mps1 in stable human cell lines reveals novel aspects of Mps1 function in mitosis. *PLoS ONE* **5**, e10251.
Tang, Z., Bharadwaj, R., Li, B. and Yu, H. (2001). Mad2-independent inhibition of APC Cdc20 by the mitotic checkpoint protein BubR1 at Dallas. *Dev. Cell* **1**, 227-237.
Uzunova, K., Dye, B. T., Schutz, H., Ladurner, R., Petzold, G., Toyoda, Y., Jarvis, M. A., Brown, N. G., Poser, I., Novatchkova, M. et al. (2012). APC15

Journal of Cell Science

mediates CDC20 autoubiquitylation by APC/C(MCC) and disassembly of the mitotic checkpoint complex. *Nat. Struct. Mol. Biol.* **19**, 1116-1123.

Van Voorhis, V. A. and Morgan, D. O. (2014). Activation of the APC/C ubiquitin ligase by enhanced E2 efficiency. *Curr. Biol.* **24**, 1556-1562.

van Zon, W., Ogink, J., ter Riet, B., Medema, R. H., te Riele, H. and Wolthuis, R. M. F. (2010). The APC/C recruits cyclin B1-Cdk1-Cks in prometaphase before D box recognition to control mitotic exit. *J. Cell Biol.* **190**, 587-602.

Vázquez-Novelle, M. D., Sansregret, L., Dick, A. E., Smith, C. A., McAinsh, A. D., Gerlich, D. W. and Petronczki, M. (2014). Cdk1 inactivation terminates mitotic checkpoint surveillance and stabilizes kinetochore attachments in anaphase. *Curr. Biol.* **24**, 638-645.

Visconti, R., Palazzo, L. and Grieco, D. (2010). Requirement for proteolysis in spindle assembly checkpoint silencing. *Cell Cycle* **9**, 564-569.

Vodermaier, H. C., Gieffers, C., Maurer-stroh, S., Eisenhaber, F. and Peters, J. (2003). TPR subunits of the anaphase-promoting complex mediate binding to the activator protein CDH1. *Curr. Biol.* **13**, 1459-1468.

Wendt, K. S., Vodermaier, H. C., Jacob, U., Gieffers, C., Gmachl, M., Peters, J. M., and Sondermann, P. (2001). Crystal structure of the APC10/DOC1 subunit of the human anaphase-promoting complex. *Nature Structural Biology*, **8**(9), 784-788.

Westhorpe, F. G., Tighe, A., Lara-Gonzalez, P. and Taylor, S. S. (2011). p31comet-mediated extraction of Mad2 from the MCC promotes efficient mitotic exit. *J. Cell Sci.* **124**, 3905-3916.

Wolthuis, R., Clay-Farrace, L., van Zon, W., Yekezare, M., Koop, L., Ogink, J., Medema, R. and Pines, J. (2008). Cdc20 and Cks direct the spindle checkpoint-independent destruction of cyclin A. *Mol. Cell* **30**, 290-302.

Wu, W., Baxter, J. E., Wattam, S. L., Hayward, D. G., Fardilha, M., Knebel, A., Ford, E. M., da Cruz e Silva, E. F. and Fry, A. M. (2007). Alternative splicing controls nuclear translocation of the cell cycle-regulated Nek2 kinase. *J. Biol. Chem.* **282**, 26431-26440.

Yudkovsky, Y., Shteinberg, M., Listovsky, T., Brandeis, M. and Hershko, A. (2000). Phosphorylation of Cdc20/fizzy negatively regulates the mammalian cyclosome/APC in the mitotic checkpoint. *Biochem. Biophys. Res. Commun.* **271**, 299-304.

Zeng, X. and King, R. W. (2012). An APC/C inhibitor stabilizes cyclin B1 by prematurely terminating ubiquitination. *Nat. Chem. Biol.* **8**, 383-392.

Zeng, X., Sigoillot, F., Gaur, S., Choi, S., Pfaff, K. L., Oh, D.-C., Hathaway, N., Dimova, N., Cuny, G. D. and King, R. W. (2010). Pharmacologic inhibition of the anaphase-promoting complex induces a spindle checkpoint-dependent mitotic arrest in the absence of spindle damage. *Cancer Cell* **18**, 382-395.